Acta Mech Sin (2010) 26:37–44
DOI 10.1007/s10409-009-0313-z

RESEARCH PAPER

Parametric study of control mechanism of cortical bone remodeling under mechanical stimulus

Yanan Wang · Qing-Hua Qin

Received: 16 June 2009 / Accepted: 3 August 2009 / Published online: 25 November 2009

Abstract The control mechanism of mechanical bone remodeling at cellular level was investigated by means of an extensive parametric study on a theoretical model described in this paper. From a perspective of control mechanism, it was found that there are several control mechanisms working simultaneously in bone remodeling which is a complex process. Typically, an extensive parametric study was carried out for investigating model parameter space related to cell differentiation and apoptosis which can describe the fundamental cell lineage behaviors. After analyzing all the combinations of 728 permutations in six model parameters, we have identified a small number of parameter combinations that can lead to physiologically realistic responses which are similar to theoretically idealized physiological responses. The results presented in the work enhanced our understanding on mechanical bone remodeling and the identified control mechanisms can help researchers to develop combined pharmacological–mechanical therapies to treat bone loss diseases such as osteoporosis.

Keywords Control mechanism · Parametric study · Mechanical bone remodeling

1 Introduction

Bone is a dynamic tissue that constantly undergoes remodeling even after growth that modeling has been completed.

Y. Wang (✉) · Q.-H. Qin
Department of Engineering, Australian National University, Canberra, ACT 0200, Australia
e-mail: yanan.wang@anu.edu.au

Q.-H. Qin
e-mail: qinghua.qin@anu.edu.au

Bone remodeling is a coupled process in which there is localized removal of old bone and replacement with newly formed bone. Followed an activation–resorption–formation sequence [1], this happens in basic multicellular unit (BMU) which is a mediator mechanism bridging individual cellular activity to whole bone morphology [2]. Two principle cell types, the osteoclast cell and osteoblast cell are found in bone, which are the main effectors in bone turnover. The osteoblast cell produces the matrix which is mineralized in a well regulated manner. The mineralized bone matrix can be removed by activated osteoclast cell. This process is complicated, requiring interaction among different cell types that are regulated by a variety of biochemical and mechanical factors. Mechanical loading is a particularly potent stimulus for bone cells, which improves bone strength and inhibits bone loss with age.

The major reason for bone remodeling is to respond and adapt to the mechanical stresses which happen as a result of mechanical loading during physical exercises. Disorder in bone remodeling is common in many bone diseases such as osteoporosis and osteoarthritis [3]. The control mechanisms responsible for the dysfunction remain unclear.

Current understanding of mechanical bone remodeling is primarily based on experimental results in vivo and in vitro. A recent report [4] shows that osteocytes are the professional mechanosensory cells of bone and the lacuno-canalicular porosity is the structure that mediates mechanosensing. It is also shown that the dynamic mechanical load causes fluid flow in the lacuno-canalicular network [5]. The experiments in vivo indicated that the fluid flow serves as the physical mediator of mechanotransduction of osteocytes [6]. It is the fluid flow shear stress [7–10] that stimulates osteocytes to produce signaling molecules within minutes [11] such as prostaglandins (especially prostaglandin E2, PGE_2) [10–17] and nitric oxide (NO) [9,13,14,18–20], which modulate the

activities of osteoblasts and osteoclasts and finish the transduction from mechanical stimuli to biochemical signaling [13]. NO is a strong inhibitor of bone resorption and acts by inhibiting the receptor activator of nuclear factor (NF)-kB ligand (RANKL) expression in osteoblast precursors and increasing osteoprotegerin (OPG) production in active osteoblasts. So it can decrease the RANKL /OPG equilibrium and reduce recruitment of osteoclasts and elevate bone formation finally [21]. Alternatively PGE_2 has strong osteogenic effects which contribute to increases in osteoblasts differentiation from marrow stromal cells through the EP_4 receptor [12,14,22–24].

The development of pharmaceutical treatment for bone diseases can be enhanced by computational models that predict their effects on bone remodeling. So far some theoretical works have been done related to mechanical bone remodeling. Huiskes et al. studied extensively on trabecular bone, ranging from prediction of development of trabecular architecture [25], to effects of mechanical forces on maintenance and adaptation of form in trabecular bone [26–29]. On the basis of trabecular bone remodeling theory developed by Weinans et al. [30], Li [31] developed a new trabecular bone remodeling model which can simulate both underload and overload resorptions that often occur in dental implant treatments. However, no control mechanism research of mechanical bone remodeling at cellular level has been done.

In this paper we investigated the underlying control mechanisms of mechanical bone remodelling system through parametric study of the theoretical model. Six fundamental differentiation and apoptosis rate parameters of the model are combined randomly with each being up and down regulated, applied as a system perturbation to the bone remodelling system. The BMC and BFE are defined as the objective criteria for assessment of each parameter combination. By using Matlab to carry out the large amount of calculations we manage to obtain 728 graphs of BMC and BFE versus model parameter combination variation as system output. After analysing all the graphs, two subsets of results are summarized. One is considered as physiologically unrealistic which consists of large amount of parameter combinations; the other one is made up of a small number of parameter combinations and presents physiologically realistic behaviour which is similar to the hypothesized ideal response. The parameter combinations that comprise latter subset of results are identified as control mechanisms and believed to be able to further our understanding of mechanical bone remodelling, and eventually help researchers to develop combined pharmacological–mechanical therapies to cure bone loss diseases.

2 Mathematical model development

Here we use abbreviation forms for the factors involved, such as OBU for uncommitted osteoblastic progenitors, OBP for preosteoblast, OBA for mature osteoblast, OCP for osteoclast precursor, OCA for active osteoclasts, OST for osteocytes, and we use RL for RANKL, RK for RANK, Tβ for TGF-β, P2 for PGE_2, OPG, NO and PTH unchanged. Also the concentration of these factors (unit: pM) is represented by the form C_{factor}, such as concentration of mature osteoblast is notated as C_{OBA}.

In modeling cell responses, the Hill Equation is often used to describe the molecular input function. The activation (act for short) and repression (rep for short) forms of the Hill equation [32] for the production rate of a new cell or molecule are [33]:

$$f(x^*) = \beta \cdot \Pi_{\text{act}} = \frac{\beta x^*}{K_1 + x^*}, \tag{1}$$

$$f(x^*) = \beta \cdot \Pi_{\text{rep}} = \frac{\beta}{1 + \frac{x^*}{K_2}}, \tag{2}$$

where x^* is the active form of concentration x which is a ligand that governs the production of a cell or molecule z through binding to its receptor on cell, β is the maximal production rate of z, and K_1 and K_2 are activation and repression coefficients. Note here that we have already assumed that Hill coefficient equals one.

The equations governing the evolution of the number of osteoblastic and osteoclastic cells in each maturation stage are simply balance equations, which means each cell stage is fed by an entering flow and is emptied by the outgoing flow of differentiated or apoptotic cells. As a result, we can formulate the mechanical bone cell population dynamics as follows:

$$\begin{aligned}\frac{\mathrm{d}C_{\text{OBP}}}{\mathrm{d}t} &= D_{\text{OBU}} \cdot \left(k_{\text{T}\beta} \cdot \Pi^{\text{T}\beta}_{\text{act,OBU}} + k_{\text{P2}} \cdot \Pi^{\text{P2}}_{\text{act,OBU}}\right) \\ &\quad - D_{\text{OBP}} \cdot C_{\text{OBP}} \cdot \Pi^{\text{T}\beta}_{\text{rep,OBP}}, \end{aligned} \tag{3}$$

$$\frac{\mathrm{d}C_{\text{OBA}}}{\mathrm{d}t} = D_{\text{OBP}} \cdot C_{\text{OBP}} \cdot \Pi^{\text{T}\beta}_{\text{rep,OBP}} - A_{\text{OBA}} \cdot C_{\text{OBA}}, \tag{4}$$

$$\frac{\mathrm{d}C_{\text{OST}}}{\mathrm{d}t} = T_{\text{OBA}} \cdot C_{\text{OBA}} - A_{\text{OST}} \cdot C_{\text{OST}}, \tag{5}$$

$$\frac{\mathrm{d}C_{\text{OCA}}}{\mathrm{d}t} = D_{\text{OCP}} \cdot \Pi^{\text{RL}}_{\text{act,OCP}} - A_{\text{OCA}} \cdot C_{\text{OCA}} \cdot \Pi^{\text{T}\beta}_{\text{act,OCA}}, \tag{6}$$

the input functions $\Pi^{\text{molecule}}_{\text{act/rep,cell}}$ are derived by using Hill equations, where "cell" means the cell type a specific molecule binds to, "molecule" denotes the ligand involved in a particular cell response and "rep/act" means repressor or activator function, for example, $\Pi^{\text{T}\beta}_{\text{act,OBU}}$, $\Pi^{\text{T}\beta}_{\text{rep,OBP}}$ and $\Pi^{\text{T}\beta}_{\text{act,OCA}}$ are the activator/repressor functions related to TGF-β binding to its receptors on osteoclasts and osteoblasts. D_{OBU} is the differentiation rate of uncommitted OB progenitors, D_{OBP} is the differentiation rate of preosteoblasts, D_{OCP} is the differentiation rate of preosteoclasts, A_{OBA} is the rate of elimination of OBA, A_{OCA} is the rate of elimination of OCA, A_{OST} is the

rate of elimination of OST. All the constants and their values can be found in Table 2 in Appendix.

Here we define a loading regime which is also widely used in animal tests [34,35]: the number of loading cycles during a training day is N, $T_{\text{rest}}(h)$ is the rest time between loading bouts, n is the number of loading bouts per day. The amplitude A (Pa) and frequency f (Hz) of the interstitial fluid shear stress (IFSS) caused by the loading can be measured using the method in Ref.[36], and therefore the peak fluid shear stress rate R_{IFSS} (Pa Hz) can be defined as [9]:

$$R_{\text{IFSS}} = 2\pi A f. \tag{7}$$

To study the sensitivity of bone remodeling to mechanical loading, we here define the mechanosensitivity of osteocytes MS_{OST} with the frequency f, number of loads per day N, the rest time between bouts T_{rest}, the length of loading period t, the time constant describing the rate at which accommodation takes place T_{acc}, the osteocyte mechanosensitivity can be written as:

$$MS_{\text{OST}} = K_{\text{MS}} \cdot \frac{\ln(f+0.5)}{N+1} \cdot \left(2 - \mathrm{e}^{-T_{\text{rest}}/\tau}\right) \cdot \mathrm{e}^{-t/T_{\text{acc}}}, \tag{8}$$

where K_{MS} is a proportionality constant.

Using Eqs. (7) and (8), based on the experimental results [8,9], we here define the concentration changes of NO and PGE_2 during bone remodeling process as:

$$\frac{\mathrm{d}C_{\text{NO}}}{\mathrm{d}t} = K_{\text{NO}} \cdot R_{\text{IFSS}} \cdot C_{\text{OST}} \cdot n \int_0^N MS_{\text{OST}} \mathrm{d}N - \tilde{D}_{\text{NO}} \cdot C_{\text{NO}}, \tag{9}$$

$$\frac{\mathrm{d}C_{\text{P2}}}{\mathrm{d}t} = K_{\text{P2}} \cdot R_{\text{IFSS}} \cdot C_{\text{OST}} \cdot n \int_0^N MS_{\text{OST}} \mathrm{d}N - \tilde{D}_{\text{P2}} \cdot C_{\text{P2}}, \tag{10}$$

K_{NO} is the secretion rate of NO by osteocytes, n is the number of loading bouts per day, K_{P2} is the secretion rate of PGE_2 by osteocytes, $\tilde{D}_{\text{NO}}$ is the rate of degradation of NO, $\tilde{D}_{\text{P2}}$ is the rate of degradation of PGE_2.

In the end we define the system output as the BMC (bone mineral content) and BFE (bone fracture energy):

$$\begin{aligned}\frac{\mathrm{dBMC}}{\mathrm{d}t} &= K_{\text{for}} \cdot [C_{\text{OBA}}(t) - C_{\text{OBA}}(t_0)] \\ &\quad - K_{\text{res}} \cdot [C_{\text{OCA}}(t) - C_{\text{OCA}}(t_0)],\end{aligned} \tag{11}$$

$$\begin{aligned}\frac{\mathrm{dBFE}}{\mathrm{d}t} &= K_{\text{for}} \cdot [C_{\text{OBA}}(t) - C_{\text{OBA}}(t_0)] \\ &\quad - K_{\text{res}} \cdot [C_{\text{OCA}}(t) - C_{\text{OCA}}(t_0)] \\ &\quad + K_{\text{to}} \cdot \sqrt{C_{\text{OBA}}(t) + C_{\text{OCA}}(t)}.\end{aligned} \tag{12}$$

Note that BMC and BFE are in percentage (%), K_{for}, K_{res} and K_{to} are the relative bone formation rate, bone resorption rate and the relative rate of bone turnover, respectively. We start the simulation from a so-called "steady-state" where BMC and BFE are 100%, $\mathrm{dBMC}/\mathrm{d}t = 0$, $\mathrm{dBFE}/\mathrm{d}t = 0$, correspondingly $C_{\text{OBA}}(t)$ is $C_{\text{OBA}}(t_0)$ and $C_{\text{OCA}}(t)$ is $C_{\text{OCA}}(t_0)$.

3 Parametric study of control mechanism

For normal adults, there is a balance between the amount of bone resorbed by osteoclasts and the amount of bone formed by osteoblasts [1]. In this complex process, bone is remodelled by groups of cells derived from different sources, which are usually called the basic multicellular units (BMUs) [37] that follow an activation–resorption–formation sequence event. The BMU is a mediator mechanism bridging individual cellular activity to whole bone morphology [2], which is sensitive to any changes in the bone cell microenvironment. As a result, it is expected that any modification to the component of BMU will have significant effect on its output behaviour. In this paper we are going to apply perturbations to the mechanical bone remodelling system which is in steady state by down and up regulating its six differentiation and apoptosis rate parameters DF_{OBU}, DF_{OCP}, DF_{OBP}, A_{OBA}, A_{OCA} and A_{OST}. In this case, we have six different parameters and each parameter could be up or down regulated, by using simple combination theory, we can calculate the number of permutation is $728 = \sum_{i=1}^{6} C_6^i \cdot 2^i$. Then in order to investigate the system behaviour for a wide range of changes, we now apply exponentially changed factor which is 1.5^{ex} to each of the six differentiation and apoptosis rate parameters, where the exponent ex ranges from -10 to 10 in step increase of 0.5. The assessment of each of the parameter combination to the system behaviour is chosen as the responses of BMC and BFE which are sampled on 100th day to stand for the maximum change. By using Matlab we can plot all the 728 graphs, then summarizing all the plots of BMC and BFE versus variation of exponent ex, we find that there are three subsets of curves which are plotted in Fig. 1.

Figure 1a and b shows an exponential increase and decrease of BMC and BFE, respectively, for increasing the model parameter exponentially (exponent ex from -10 to 10). This type of behaviour is considered as physiological unrealistic from a biological viewpoint and obtained for a quite large range of model parameter combinations. On the other hand, Fig. 1c represents the other extreme case where only minor changes of BMC and BFE happen during the entire range of parameter variation. These three types of response curves are excluded from our further analysis on the grounds that they do not provide an effective control mechanism for BMC and BFE.

In Ref. [33] the "idealized" regulatory response by functionally active BMUs is discussed. As we stated earlier, the bone remodelling system is started from a steady state where

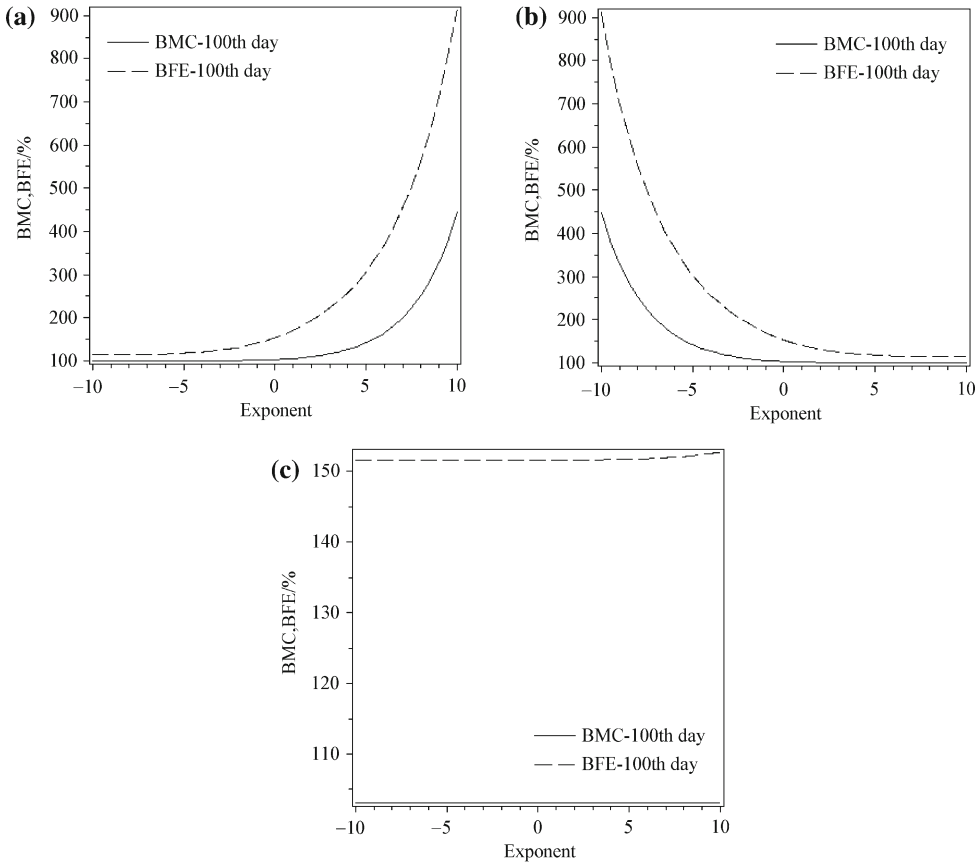

Fig. 1 Physiological unrealistic changes of BMC and BFE versus combined changes of model parameter $[1.5^{-10} - 1.5^{+10}] \cdot p$. **a** Exponential bone growth; **b** exponential bone decrease; **c** slight changes of bone (p is parameter value)

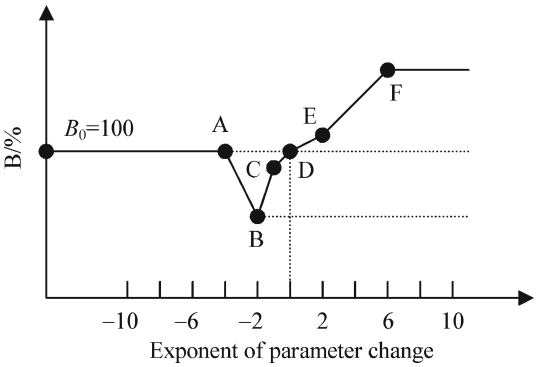

Fig. 2 Schematic illustration of ideal response curve for combined changes of model parameters

we can identify $\Delta\text{BMC} = 0$, $\Delta\text{BFE} = 0$, and concentrations of various hormones, growth factors and so on that cause initial values of differentiation and apoptosis rates in BMUs. In order to respond to minor changes in concentrations it is expected that BMUs should be rather insensitive to these fluctuations. Therefore from Fig. 2 we can recognize point A as the threshold concentration, which means any change of model parameter underneath A causes no change in BMC (/BFE). Also, a region around the usual operation status of BMUs should be found with relatively small gradients of changes in BMC (/BFE) in response to changes in differentiation rates (regions C–D and D–E in Fig. 2), with larger gradients for larger changes in differentiation rates (region E–F in Fig. 2). Though it is expected to see that this response in BMC (/BFE) change to remain limited if the differentiation rates increase significantly (region further after point F in Fig. 2), because the BMC (/BFE) rising unlimitedly is not physiologically realistic. On the other hand, it is expected that the rate of BMC (/BFE) change would also decrease limitedly if the differentiation rates decrease significantly. As a matter of fact, physiologically it is reasonable for the BMC (/BFE) change to be zero for extremely small differentiation rates. Additionally it can be seen that from Fig. 2 point F marks the maximum change in BMC (/BFE) (ΔB max). Since we have point A which is the maximum concentration that does not lead to further modifications of BMC (/BFE), there must be a transition region from point C to point A which is characterized by point B the lowest value of BMC (/BFE).

After having found a potential "ideal response curve", we can now start searching for response curves that may meet these requirements. Encouragingly, we have been able to identify a small number of curves that possess similarity to the idealised response curve. Table 1 summarizes all the parameter combinations that produce idealized response

Table 1 Summary of parameter combinations that lead to controlled remodelling process

Number of parameters in a combination	Combinations of differentiation and apoptosis rates	Variation of each parameter
1	A_{OBA}	$-$
1	A_{OST}	$-$
2	D_{OBP}/A_{OBA}	$+/-$
2	D_{OBP}/A_{OST}	$-/-$
2	D_{OCP}/A_{OBA}	$-/-$
2	D_{OCP}/A_{OST}	$-/-$
2	A_{OBA}/A_{OCA}	$-/+$
2	A_{OCA}/A_{OST}	$+/-$
3	$D_{OBP}/D_{OCP}/A_{OBA}$	$-/-/-$
3	$D_{OBP}/D_{OCP}/A_{OBA}$	$-/+/-$
3	$D_{OBP}/A_{OBA}/A_{OCA}$	$-/-/-$
3	$D_{OBP}/A_{OBA}/A_{OCA}$	$-/-/+$
3	$D_{OBP}/A_{OBA}/A_{OST}$	$-/-/-$
3	$D_{OBP}/A_{OBA}/A_{OST}$	$+/-/+$
3	$A_{OBA}/A_{OCA}/A_{OST}$	$-/+/+$
4	$D_{OBU}/D_{OBP}/A_{OBA}/A_{OST}$	$+/+/+/-$
4	$D_{OBP}/D_{OCP}/A_{OBA}/A_{OCA}$	$-/-/-/-$
4	$D_{OBP}/D_{OCP}/A_{OBA}/A_{OCA}$	$-/-/-/+$
4	$D_{OBU}/D_{OCP}/A_{OBA}/A_{OST}$	$-/+/-/-$
4	$D_{OBP}/A_{OBA}/A_{OCA}/A_{OST}$	$-/-/+/-$
4	$D_{OBP}/A_{OBA}/A_{OCA}/A_{OST}$	$+/-/-/+$
5	$D_{OBU}/D_{OBP}/D_{OCP}/A_{OBA}/A_{OST}$	$-/-/+/-/-$
5	$D_{OBU}/D_{OBP}/D_{OCP}/A_{OBA}/A_{OST}$	$+/-/-/+/-$
5	$D_{OBU}/D_{OBP}/A_{OBA}/A_{OCA}/A_{OST}$	$-/+/-/-/-$
5	$D_{OBU}/D_{OBP}/A_{OBA}/A_{OCA}/A_{OST}$	$+/-/+/+/-$
5	$D_{OBP}/D_{OCP}/A_{OBA}/A_{OCA}/A_{OST}$	$-/+/-/-/-$
5	$D_{OBP}/D_{OCP}/A_{OBA}/A_{OCA}/A_{OST}$	$-/-/-/+/-$
5	$D_{OBP}/D_{OCP}/A_{OBA}/A_{OCA}/A_{OST}$	$-/-/-/-/+$
6	$D_{OBU}/D_{OBP}/D_{OCP}/A_{OBA}/A_{OCA}/A_{OST}$	$+/-/-/+/-/-$
6	$D_{OBU}/D_{OBP}/D_{OCP}/A_{OBA}/A_{OCA}/A_{OST}$	$+/-/-/+/+/-$

The variation with "+" represents parameter increase, "−" represents parameter decrease

curves. In Fig. 3 we plot the physiologically realistic response curve which corresponds to the parameter permutation involving three parameters ($A_{OBA}/A_{OCA}/A_{OST} = -/+/+$) and is similar to the idealised response curve shown in Fig. 2.

It is noticed that in a bone remodelling system without consideration of mechanical stimulus, the response involving three parameters (that is $D_{OBU}/D_{OBP}/A_{OCA} = +/-/+$) coincides with the known physiological action of TGF-β on bone cells that TGF-β promotes differentiation of osteoblast progenitors, inhibits differentiation of osteoblast precursor cells, while promoting of osteoclast apoptosis [33]. But in the case of mechanical bone remodelling this combination causes exponential increases for both BMC and BFE, which is similar to Fig. 1a. In other words, with the introduction of mechanical stimulus the bone remodelling system becomes different and it deserves attention from biologists and other researchers as well.

4 Summary and conclusion

In this paper, based on our previous work, the parametric study of mechanical bone remodeling model is carried out in order to understand the control mechanism of mechanical bone remodeling at cellular level. From a control mechanism perspective, it is quite likely that there are several control mechanisms working simultaneously in bone remodeling which is a complex system. Consequently, we perform an extensive parametric study investigating model parameter space related to cell differentiation and apoptosis which

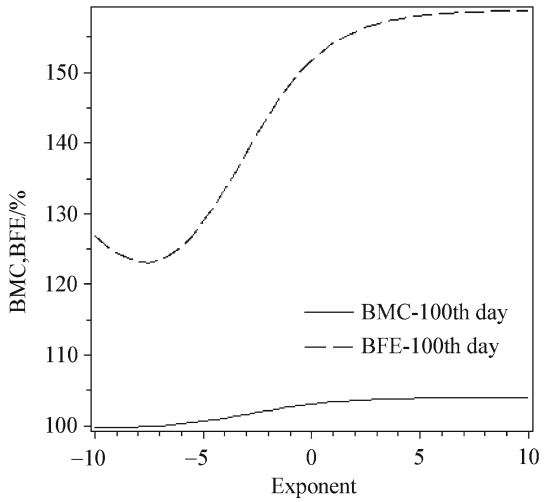

Fig. 3 Typical physiologically realistic fluctuations of BMC and BFE with combinations of parameter change

describes the fundamental cell lineage behaviors, to investigate such a scenario. After analyzing all the combinations (which are 728 permutations) of six model parameters, we successfully identified a small number of parameter combinations that are able to cause physiologically realistic responses which are similar to theoretically idealized physiological response. In the end, this work will further our understanding on mechanical bone remodeling and the identified control mechanisms are able to help to develop combined pharmacological and mechanical therapies to treat bone loss diseases such as osteoporosis.

Appendix

See Table 2.

Table 2 Parameter values and descriptions [17,26]

Symbol	Unit	Value	Description
D_{OBU}	pM/day	7×10^{-4}	Differentiation rate of uncommitted OB progenitors
D_{OBP}	pM/day	5.348	Differentiation rate of preosteoblasts
D_{OCP}	pM/day	2.1×10^{-3}	Differentiation rate of preosteoclasts
A_{OBA}	pM/day	1.890×10^{-1}	Rate of elimination of OBA
A_{OCA}	pM/day	7.000×10^{-1}	Rate of elimination of OCA
A_{OST}	pM/day	3.1×10^{-2}	Rate of elimination of OST
$K_{\mathrm{D1,T}\beta}$	pM	4.545×10^{-3}	Activation coefficient related to TGF-β binding on OBU
$K_{\mathrm{D2,T}\beta}$	pM	1.416×10^{-3}	Repression coefficient related to TGF-β binding on OBP
$K_{\mathrm{D3,T}\beta}$	pM	4.545×10^{-3}	Activation coefficient of TGF-β binding on OCA
$K_{\mathrm{D4,PTH}}$	pM	1.500×10^{2}	Activation coefficient for $\mathrm{RANKL_{eff}}$ on OBP related to PTH binding
$K_{\mathrm{D5,PTH}}$	pM	2.226×10^{-1}	Repression coefficient for OPG production related to PTH binding on OBA
$K_{\mathrm{D6,RL}}$	pM	1.500×10^{2}	Activation coefficient related to RANKL binding on OCP
$K_{\mathrm{D7,NO}}$	pM	1.573×10	Activation coefficient for OPG production on OBA related to NO
$K_{\mathrm{D8,NO}}$	pM	2.189×10	Repression coefficient for RANKL production on OBP related to NO
$K_{\mathrm{D9,P2}}$	pM	3.674	Activation coefficient for OBU differentiation related to $\mathrm{PGE_2}$
RK	pM	1×10	Unchanged concentration of RANK
R_{RL}	–	3×10^{6}	Maximum RANKL on OBP
β_{PTH}	pM/cell	2.5×10^{2}	Synthesis rate of systemic PTH
β_{RL}	pM/cell	1.684×10^{4}	Production rate of RANKL per OBP
β_{OPG}	pM/cell	1.464×10^{8}	Production rate of OPG per OBA
$\tilde{D}_{\mathrm{PTH}}$	pM/day	8.6×10	Rate of degradation of PTH
$\tilde{D}_{\mathrm{RL}}$	pM/cell	1.013×10	Rate of degradation of RANKL
$\tilde{D}_{\mathrm{OPG}}$	pM/cell	3.5×10^{-1}	Rate of degradation of OPG
$\tilde{D}_{\mathrm{T}\beta}$	pM/cell	1×10^{0}	Rate of degradation of TGF-β
$\tilde{D}_{\mathrm{NO}}$	pM/cell	1×10^{3}	Rate of degradation of NO
$\tilde{D}_{\mathrm{P2}}$	pM/cell	1×10^{2}	Rate of degradation of T $\mathrm{PGE_2}$
$k_{\mathrm{T}\beta}$	–	0.5	Relative influence of TGF-β binding in OBU differentiation

Table 2 continued

Symbol	Unit	Value	Description
k_{P2}	–	0.5	Relative influence of PGE_2 in OBU differentiation
k_{PTH}	–	0.7	Relative influence of PTH binding in production of OPG in OBA
k_{NO}	–	0.3	Relative influence of NO in production of OPG in OBA
$K_{A1,RL}$	pM^{-1}	1×10^{-3}	Association binding constant RANKL-OPG
$K_{A2,RL}$	pM^{-1}	3.412×10^{-2}	Association binding constant RANKL-RANK
OPG_{max}	pM	2×10^{8}	Maximum possible OPG concentration
α	%	1	TGF-β content stored in bone matrix
K_{res}	day^{-1}	1	Relative rate of bone resorption
K_{for}	day^{-1}	1.571	Relative rate of bone formation
K_{to}	day^{-1}	1.552×10	Relative rate of bone turnover
T_{OBA}	pM/day	0.15	Rate of trapped OBA in bone matrix
K_{NO}	pM/day	2×10^{4}	Secretion rate of NO by osteocytes
K_{P2}	pM/day	1×10^{2}	Secretion rate of PGE_2 by osteocytes

References

1. Robling, A.G., Castillo, A.B., Turner, C.H.: Biomechanical and molecular regulation of bone remodeling. Annu. Rev. **8**, 455–498 (2006)
2. Frost, H.M.: Intermediary Organization of the Skeleton. CRC Press, Boca Raton (1986)
3. Moroz, A., Crane, M.C., Smith, G., Wimpenny, D.I.: Phenomenological model of bone remodeling cycle containing osteocyte regulation loop. Biosystems **84**, 183–190 (2006)
4. Nijweide, P.J., Burger, E.H., Klein-Nulend, J.: The Osteocyte. Academic Press, San Diego (2002)
5. Knothe Tate, M.L., Steck, R., Forwood, M.R., Niederer, P.: In vivo demonstration of load-induced fluid flow in the rat tibia and its potential implications for processes associated with functional adaptation. J. Exp. Biol. **203**, 2737–2745 (2000)
6. Weinbaum, S., Cowin, S.C., Zeng, Y.: A model for the excitation of osteocytes by mechanical loading-induced bone fluid shear stresses. J. Biomech. **27**, 339–360 (1994)
7. Klein-Nulend, J., Bacabac, R.G., Mullender, M.G.: Mechanobiology of bone tissue. Pathol. Biol. **53**, 576–580 (2005)
8. Bakker, A.D., Soejima, K., Klein-Nulend, J., Burger, E.H.: The production of nitric oxide and prostaglandin E2 by primary bone cells is shear stress dependent. J. Biomech. **34**, 671–677 (2001)
9. Bacabac, R.G., Smit, T.H., Mullender, M.G., Dijcks, S.J., Loon, J.J.V., Klein-Nulend, J.: Nitric oxide production by bone cells is fluid shear stress rate dependent. Biochem. Biophys. Res. Commun. **315**, 823–829 (2004)
10. Mullender, M., El Haj, A., Yang, Y., van Duin, M., Burger, E., Klein-Nulend, J.: Mechanotransduction of bone cellsin vitro: mechanobiology of bone tissue. Med. Biol. Eng. Comput. **42**, 14–21 (2004)
11. Ajubi, N.E., Klein-Nulend, J., Nijweide, P.J., Vrijheid-Lammers, T., Alblas, M.J., Burger, E.H.: Pulsating fluid flow increases prostaglandin production by cultured chicken osteocytes-a cytoskeleton-dependent process. Biochem. Biophys. Res. Commun. **225**, 62–68 (1996)
12. Ajubi, N.E., Klein-Nulend, J., Alblas, M.J., Burger, E.H., Nijweide, P.J.: Signal transduction pathways involved in fluid flow-induced PGE2 production by cultured osteocytes. Am. J. Physiol. Endocrinol. Metab. **276**, E171–E178 (1999)
13. Burger, E.H., Klein-Nulend, J.: Mechanotransduction in bone-role of the lacuno-canalicular network. FASEB J. **13**, 101–112 (1999)
14. Chambers, T.J., Fox, S., Jagger, C.J., Lean, J.M., Chow, J.W.M.: The role of prostaglandins and nitric oxide in the response of bone to mechanical forces. Osteoarthr. Cartil. **7**, 422–423 (1999)
15. Bakker, A., Klein-Nulend, J., Burger, E.: Mechanotransduction in bone cells proceeds via activation of COX-2, but not COX-1. Biochem. Biophys. Res. Commun. **305**, 677–683 (2003)
16. Joldersma, M., Klein-Nulend, J., Oleksik, A.M., Heyligers, I.C., Burger, E.H.: Estrogen enhances mechanical stress-induced prostaglandin production by bone cells from elderly women. Am. J. Physiol. Endocrinol. Metab. **280**, E436–E442 (2001)
17. Klein-Nulend, J., Sterck, J.G.H., Sterck, J.G.H., Semeins, C.M., Lips, P., Joldersma, M., Baart, J.A., Burger, E.H.: Donor age and mechanosensitivity of human bone cells. Osteoporosis Int. **13**, 137–146 (2002)
18. Wang, F.S., Wang, C.J., Chen, Y.J., Huang, Y.T., Huang, H.C., Chang, P.R., Sun, Y.C., Yang, K.D.: Nitric oxide donor increases osteoprotegerin production and osteoclastogenesis inhibitory activity in bone marrow stromal cells from ovariectomized rats. Endocrinology **145**, 2148–2156 (2004)
19. Burger, E.H., Klein-Nulend, J., Smit, T.H.: Strain-derived canalicular fluid flow regulates osteoclast activity in a remodelling osteon-proposal. J. Biomech. **36**, 1453–1459 (2003)
20. van'T Hof, R.J., Ralston, S.H.: Nitric oxide and bone. Immunology **103**, 255–261 (2001)
21. Fan, X., Roy, E., Zhu, L., Murphy, T.C., Ackert-Bicknell, C., Hart, C.M., Rosen, C., Nanes, M.S., Rubin, J.: Nitric oxide regulates receptor activator of nuclear factor-{kappa}B ligand and osteoprotegerin expression in bone marrow stromal cells. Endocrinology **145**, 751–759 (2004)
22. Machwate, M., Harada, S., Leu, C.T., Seedor, G., Labelle, M., Gallant, M., Hutchins, S., Lachance, N., Sawyer, N., Slipetz, D., Metters, K.M., Rodan, S.B., Young, R., Rodan, G.A.: Prostaglandin receptor EP4 mediates the bone anabolic effects of PGE2. Mol. Pharmacol. **60**, 36–41 (2001)
23. Keila, S., Kelner, A., Weinreb, M.: Systemic prostaglandin E2 increases cancellous bone formation and mass in aging rats and stimulates their bone marrow osteogenic capacity in vivo and in vitro. J. Endocrinol. **168**, 131–139 (2001)
24. Raisz, L.G.: Physiology and pathophysiology of bone remodeling. Clin. Chem. **45**, 1353–1358 (1999)

25. Mullender, M.G., Huiskes, R., Weinans, H.: A physiological approach to the simulation of bone remodeling as a self organization control process. J. Biomech. **27**, 1389–1394 (1994)
26. Huiskes, R., Ruimerman, R., van Lenthe, G.H., Janssen, J.D.: Effects of mechanical forces on maintenance and adaptation of form in trabecular bone. Nature **405**, 704–706 (2000)
27. Ruimerman, R., Huiskes, R., van Lenthe, G.H., Janssen, J.D.: A computer-simulation model relating bone-cell metabolism to mechanical adaptation of trabecular architecture. Comput Methods Biomech. Biomed. Eng. **4**, 433–448 (2001)
28. Ruimerman, R., Hilbers, P., van Rietbergen, B., Huiskes, R.: A theoretical framework for strain-related trabecular bone maintenance and adaptation. J. Biomech. **38**, 931–941 (2005)
29. Ruimerman, R.: Modeling and remodeling in bone tissue. Technische Universiteit Eindhoven, Eindhoven. http://alexandria.tue.nl/extra2/200510655.pdf (2005)
30. Weinans, H., Huiskes, R., Grootenboer, H.J.: The behavior of adaptive bone-remodeling simulation models. J. Biomech. **25**, 1425–1441 (1992)
31. Li, J., Li, H., Shi, L., Fok, A.S.L., Ucer, C., Devlin, H., Horner, K., Silikas, N.: A mathematical model for simulating the bone remodeling process under mechanical stimulus. Dent. Mater. **23**, 1073–1078 (2007)
32. Alon, U.: An Introduction to Systems Biology: Design Principles of Biological Circuits. CRC Press, New York (2007)
33. Pivonka, P., Zimak, J., Smith, D.W., Gardiner, B.S., Dunstan, C.R., Sims, N.A., John Martin, T., Mundy, G.R.: Model structure and control of bone remodeling: a theoretical study. Bone **43**, 249–263 (2008)
34. Robling, A.G., Hinant, F.M., Burr, D.B., Turner, C.H.: Improved bone structure and strength after long-term mechanical loading is greatest if loading is separated into short bouts. J. Bone Miner. Res. **17**, 1545–1554 (2002)
35. Rubin, C., Turner, A.S., Bain, S., Mallinckrodt, C., McLeod, K.: Anabolism. Low mechanical signals strengthen long bones. Nature **412**, 603–604 (2001)
36. Bergmann, G., Graichen, F., Rohlmann, A.: Hip joint force measurements. http://www.medizin.fu-berlin.de/biomechanik/homefrme.htm (2003)
37. Parfitt, A.M.: Osteonal and hemi-osteonal remodeling: the spatial and temporal framework for signal traffic in adult human bone. J. Cell. Biochem. **55**, 273–286 (1994)